
Mamba MethaneMapper: State Space Model for Methane Detection from Hyperspectral Imagery

Satish Kumar¹
satishkumar@ucsb.edu

ASM Iftekhar¹
iftekhar@ucsb.edu

Bowen Zhang¹
bowen68@ucsb.edu

Kaikai Liu¹
kaikailiu@ucsb.edu

Mehan Jayasuriya
mehan@mozillafoundation.org
Mozilla Foundation

¹University of California Santa Barbara

Abstract

Methane (CH_4) is the chief contributor to global climate change. Recent advancements in AI-based image processing have paved the way for innovative approaches for the detection of methane using hyperspectral imagery. Existing methods, while effective, often come with high computational demands and associated costs that can limit their practical applications. Addressing these limitations, we propose the Mamba MethaneMapper (MMM), a cost-effective and efficient AI-driven solution designed to enhance methane detection capabilities in hyperspectral images. MMM will incorporate two key innovations that collectively improve performance while managing costs. First, we will utilize a gpu-aware state-space encoder, which optimizes the computational resources and efficiency of the system. Second, MMM will use an environment-sensitive module to prioritize image regions likely containing methane emissions, which are then analyzed by our efficient Mamba algorithm. This selective approach not only improves the accuracy of methane detection but also significantly reduces unnecessary computations and memory consumption.

1 Introduction

We address the challenge of detecting and pinpointing methane (CH_4) plumes using multispectral and hyperspectral imaging data as an object detection and segmentation problem. Identifying and locating potential methane emission hot spots is a crucial initial step in mitigating global warming caused by greenhouse gases. Methane is responsible for approximately 20% of the global warming effect attributed to greenhouse gases [9]. Its Global Warming Potential (GWP) is 86 times greater than that of carbon dioxide (CO_2) over a 20-year timeframe [17]. This underscores the urgent need to monitor and reduce methane emissions. Methane persists in the atmosphere for an average of 7.9 years [16], and its atmospheric concentration has been rising steadily since the industrial revolution [1]. While the annual increase in methane levels slowed between 1999 and 2006, it began to rise again in 2007 [18].

While methane emission has many sources, the ones of particular interest are those from oil and natural gas industries. According to the United States Environmental Protection Agency report, methane emissions from these industries accounts to 84 million tons per year [7, 13]. Current efforts to detect these sources mostly depend on aerial imagery. The Jet Propulsion Laboratory (JPL) has conducted thousands of aerial surveys in the last decade to collect data using an airborne sensor AVIRIS-NG [8]. Several methods have been proposed to detect potential emission sites from such imagery, for example, see [19, 20, 2, 12, 14, 10]. Most existing methods exhibit high sensitivity to background context and variations in land-cover types, which leads to a substantial number of false positives. These false detections typically require considerable intervention from domain experts

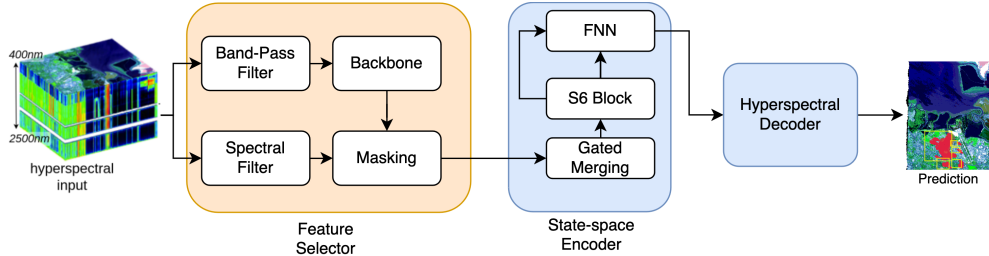


Figure 1: *Overview of the MMM architecture: The hyperspectral image input will be processed through a feature selector block. A band-pass filter will isolate the salient bands within the RGB (400-700nm) and SWIR (2000-2500nm) channels. These isolated channels will be fed into the backbone feature extractor. The spectral filter will identify potential methane regions, which will be used as masks to select specific spatial locations in the extracted features. These features will then be encoded by the state-space encoder and decoded by the hyperspectral decoder to predict bounding boxes and segmentation masks for methane detection. FNN and S6 refer as the feed-forward network and the Mamba state-space block, respectively.*

to correct. Kumar et al. [14, 12, 10] addressed these limitations by developing a neural network architecture capable of modeling background distributions to suppress false positives. Their work introduced a hyperspectral transformer model, guided by queries containing prior information about methane hotspots, facilitating accurate feature extraction and achieving state-of-the-art detection performance.

However, despite the accuracy of these models, they rely on transformer architecture with attention mechanisms that are computationally inefficient [3, 11, 15]. Attention layers introduce significant overhead in both computational complexity and inference time. To mitigate these inefficiencies, we propose Mamba MethaneMapper (MMM), a novel framework that replaces the attention mechanism in the transformer architectures with a Mamba-S6 [3] state space block. This block reduces the quadratic computational complexity of the attention mechanisms to linear complexity. However, due to the nature of the hyperspectral data just replacing attention mechanism will not render to an efficient architecture[22]. Therefore, we propose an environment dependent selection strategy in the form of feature selector block.

In summary, MMM will incorporate two primary innovative modules. First, it will integrate a GPU-optimized state-space encoder [3], which is designed to maximize computational efficiency. Second, MMM will employ an environment-adaptive feature selector to select regions that are likely to contain methane emissions. These prioritized regions will then be processed the mentioned encoder, reducing unnecessary computations and memory usage.

2 Mamba MethaneMapper Architecture

Data Overview For initial development and preliminary exploration, we will use the Methane Hot Spots (MHS) dataset [10]. We will train and test on the subset of the dataset from 2015. This subset includes flightlines from the Four-Corner (New Mexico, Arizona, Utah, and Colorado) region in United States of America. The dataset contains approximately 114 flightlines with point source emissions. We excluded the diffused emission source for the initial experiments. AVIRIS-NG hyperspectral imaging sensors capture spectral radiance values from N_0 ($N_0 = 432$) channels corresponding to wavelengths ranging from $400nm - 2500nm$. The complete hyperspectral image is represented as $\mathbf{x} \in \mathbb{R}^{H_0 \times W_0 \times N_0}$ where H_0, W_0 are the height & width, respectively, and $N_0 = 432$ is the number of channels.

2.1 Technical Overview

As can be seen in 1, MMM composed of the following components: 1) Feature Selector block to extract and selects salient features from the input hyperspectral image. 2) State-space Encoder to encode the selected features via Mamba-S6 state-space block. 3) Hyperspectral decoder to decode

the encoded feature map into segmentation mask and bounding boxes. Our Hyperspectral decoder follows the same architecture as the previous work[10]. Due to space constraints, we will just give overview to the Feature selector and the state-space encoder.

Feature selector The feature selector takes hyperspectral images as input. Since not all wavelengths are relevant for methane detection, we selectively pass only the most useful channels for feature extraction. The band-pass filter block achieves this by employing separate filters for the RGB (400nm-700nm) and SWIR(2000nm-2500nm) channels. These filtered channels are then concatenated for feature extraction by the backbone, which can be any standard feature extractor, such as ResNet [6].

Our spectral filter operates alongside the band-pass filter and the backbone. As input it takes the full hyperspectral image. Utilizing a matched filter, it leverages the methane absorption pattern to identify potential regions containing methane gas (see [10] for more details). This method has high recall but poor precision, therefore, we will use it to select potential methane containing regions in the hyperspectral images. Our masking block will use these identified regions to determine which parts of the extracted features will be passed to the encoder block, discarding the rest. The amount of discarding will be determined empirically.

State-Space Encoder The state-space encoder receives the selected features from the feature extractor block. It adheres to a traditional encoder architecture [21] but replaces the attention mechanism with the Mamba-S6 block. State-space models [4, 5] are known for their computational efficiency in sequence modeling. However, they typically lack context awareness due to fixed input parameters. The recent GPU-aware Mamba-S6 block [3] addresses this limitation. We will integrate this block into our state-space encoder. Additionally, a gated merging mechanism will be incorporated to group nearby spatial locations in the features, further reducing the number of input sequences to the Mamba-S6 block. The merging mechanism will have depth-wise and pixel-wise convolution inspired from the recent work [22].

As mentioned earlier, Hyperspectral decoder will follow the traditional design [10]. It will utilize feed-forward networks and de-convolution to predict bounding boxes and segmentation masks respectively.

3 Experimental Setup & Preliminary Analysis

We will use the MHS dataset [10] to train and test the model. We will evaluate the quality of our model following the evaluation protocol of H-mrcnn[14].

Our initial implementation of the model has demonstrated a fourfold reduction in training memory usage. As development progresses, we anticipate achieving even greater efficiency. Unlike existing works [14, 10], which primarily emphasize accuracy without considering computational costs, our approach balances both. We build on the inherent efficiency of state-space models while enhancing it with our environment-sensitive feature selector. This selector further reduces computational overhead, allowing us to deliver a model that is not only highly accurate, but also computationally efficient.

4 Conclusion

In this proposal, we propose an end-to-end methane detection model, MMM. MMM has two unique modules that leverage GPU-aware state-space model along with environment specific filter to detect methane in an efficient manner. The successful implementation of MMM will pave the way for large-scale deployment of real-time methane monitoring systems, enabling more effective and widespread environmental monitoring.

References

- [1] Philippe Ciais, Christopher Sabine, Govindasamy Bala, Laurent Bopp, Victor Brovkin, Josep Canadell, Abha Chhabra, Ruth DeFries, James Galloway, Martin Heimann, et al. Carbon and other biogeochemical cycles. In *Climate change 2013: the physical science basis. Contribution of Working Group I to the Fifth Assessment Report of the Intergovernmental Panel on Climate Change*, pages 465–570. Cambridge University Press, 2014.

- [2] Christian Frankenberg, Andrew K Thorpe, David R Thompson, Glynn Hulley, Eric Adam Kort, Nick Vance, Jakob Borchardt, Thomas Krings, Konstantin Gerilowski, Colm Sweeney, et al. Airborne methane remote measurements reveal heavy-tail flux distribution in four corners region. *Proceedings of the national academy of sciences*, 113(35):9734–9739, 2016.
- [3] Albert Gu and Tri Dao. Mamba: Linear-time sequence modeling with selective state spaces. *arXiv preprint arXiv:2312.00752*, 2023.
- [4] Albert Gu, Tri Dao, Stefano Ermon, Atri Rudra, and Christopher Ré. Hippo: Recurrent memory with optimal polynomial projections. *Advances in neural information processing systems*, 33:1474–1487, 2020.
- [5] Albert Gu, Karan Goel, and Christopher Ré. Efficiently modeling long sequences with structured state spaces. *arXiv preprint arXiv:2111.00396*, 2021.
- [6] Kaiming He, Xiangyu Zhang, Shaoqing Ren, and Jian Sun. Deep residual learning for image recognition. In *Proceedings of the IEEE conference on computer vision and pattern recognition*, pages 770–778, 2016.
- [7] Paris IEA. Methane from oil & gas, 2020.
- [8] California Institute of Technology Jet Propulsion Laboratory. Airborne visible infrared imaging spectrometer - next generation (aviris-ng) overview, 2009.
- [9] Stefanie Kirschke, Philippe Bousquet, Philippe Ciais, Marielle Saunois, Josep G Canadell, Edward J Dlugokencky, Peter Bergamaschi, Daniel Bergmann, Donald R Blake, Lori Bruhwiler, et al. Three decades of global methane sources and sinks. *Nature geoscience*, 6(10):813–823, 2013.
- [10] Satish Kumar, Ivan Arevalo, ASM Iftekhar, and BS Manjunath. Methanemapper: Spectral absorption aware hyperspectral transformer for methane detection. In *Proceedings of the IEEE/CVF Conference on Computer Vision and Pattern Recognition*, pages 17609–17618, 2023.
- [11] Satish Kumar, ASM Iftekhar, Ekta Prashnani, and BS Manjunath. LoCl: Learning object-attribute composition using localization. *arXiv preprint arXiv:2210.03780*, 2022.
- [12] Satish Kumar, William Kingwill, Rozanne Mouton, Wojciech Adamczyk, Robert Huppertz, and Evan D Sherwin. Guided transformer network for detecting methane emissions in sentinel-2 satellite imagery. In *NeurIPS 2022 Workshop on Tackling Climate Change with Machine Learning*, 2022.
- [13] Satish Kumar, Rui Kou, Henry Hill, Jake Lempges, Eric Qian, and Vikram Jayaram. In-situ water quality monitoring in oil and gas operations. *arXiv preprint arXiv:2301.08800*, 2023.
- [14] Satish Kumar, Carlos Torres, Oytun Ulutan, Alana Ayasse, Dar Roberts, and BS Manjunath. Deep remote sensing methods for methane detection in overhead hyperspectral imagery. In *Proceedings of the IEEE/CVF Winter Conference on Applications of Computer Vision*, pages 1776–1785, 2020.
- [15] Satish Kumar, Bowen Zhang, Chandrakanth Gudavalli, Connor Levenson, Lacey Hughey, Jared A Stabach, Irene Amoke, Gordon Ojwang, Joseph Mukeka, Stephen Mwiu, et al. Wildlifemapper: Aerial image analysis for multi-species detection and identification. In *Proceedings of the IEEE/CVF Conference on Computer Vision and Pattern Recognition*, pages 12594–12604, 2024.
- [16] JOS Lelieveld, Paul J Crutzen, and Frank J Dentener. Changing concentration, lifetime and climate forcing of atmospheric methane. *Tellus B*, 50(2):128–150, 1998.
- [17] Gunnar Myhre, Drew Shindell, and Julia Pongratz. Anthropogenic and natural radiative forcing. 2014.
- [18] Euan G Nisbet, Edward J Dlugokencky, and Philippe Bousquet. Methane on the rise—again. *Science*, 343(6170):493–495, 2014.
- [19] DR Thompson, I Leifer, H Bovensmann, M Eastwood, M Fladeland, C Frankenberg, K Gerilowski, RO Green, S Kratwurst, T Krings, et al. Real-time remote detection and measurement for airborne imaging spectroscopy: a case study with methane. *Atmospheric Measurement Techniques*, 8(10):4383–4397, 2015.
- [20] Andrew K Thorpe, Christian Frankenberg, David R Thompson, Riley M Duren, Andrew D Aubrey, Brian D Bue, Robert O Green, Konstantin Gerilowski, Thomas Krings, Jakob Borchardt, et al. Airborne doas retrievals of methane, carbon dioxide, and water vapor concentrations at high spatial resolution: application to aviris-ng. *Atmospheric Measurement Techniques*, 10(10):3833–3850, 2017.
- [21] Ashish Vaswani, Noam Shazeer, Niki Parmar, Jakob Uszkoreit, Llion Jones, Aidan N Gomez, Łukasz Kaiser, and Illia Polosukhin. Attention is all you need. *Advances in neural information processing systems*, 30, 2017.
- [22] Jing Yao, Danfeng Hong, Chenyu Li, and Jocelyn Chanussot. Spectralmamba: Efficient mamba for hyperspectral image classification. *arXiv preprint arXiv:2404.08489*, 2024.